UNLV | UNIVERSITY LIBRARIES

8-1-2018

Efficacy of Combined 5-Fluorouracil and Photodynamic Therapy in Glioma Spheroids

Karanjit Singh

Follow this and additional works at: https://digitalscholarship.unlv.edu/thesesdissertations

Part of the Medicine and Health Sciences Commons

www.manaraa.com

EFFICACY OF COMBINED 5-FLUOROURACIL AND PHOTODYNAMIC THERAPY IN

GLIOMA SPHEROIDS

By

Karanjit Singh

Bachelor of Science in Biomedical Physics

Wayne State University, Michigan

2013

A thesis submitted in partial fulfillment

of the requirements for the

Master of Science – Health Physics

Department of Health Physics and Diagnostic Sciences

School of Allied Health Sciences

Division of Health Sciences

The Graduate College

University of Nevada, Las Vegas

August 2018

Thesis Approval

The Graduate College
The University of Nevada, Las Vegas

May 24, 2018

This thesis prepared by

Karanjit Singh

entitled

Efficacy of Combined 5-Fluorouracil and Photodynamic Therapy in Glioma Spheroids

is approved in partial fulfillment of the requirements for the degree of

Master of Science – Health Physics
Department of Health Physics and Diagnostic Sciences

Steen Madsen, Ph.D.   Kathryn Hausbeck Korgan, Ph.D.
Examination Committee Chair   *Graduate College Interim Dean*

Francis Cucinotta, Ph.D.
Examination Committee Member

Yu Kuang, Ph.D.
Examination Committee Member

Henry Hirschberg, M.D.
Examination Committee Member

Jing Nong Liang, Ph.D.
Graduate College Faculty Representative

ii

ABSTRACT

Standard treatment regimens consisting of surgery, radiation and chemotherapy have proven ineffective for the treatment of high-grade gliomas such as glioblastoma multiforme (GBM). An effective cure requires elimination of nests of tumor cells that have migrated from the resection margin and infiltrated normal brain. A number of localized therapies, including light-based approaches such as photodynamic therapy (PDT) and photochemical internalization (PCI) are currently under investigation for the management of GBM patients.

Several studies have demonstrated a high degree of synergy between PDT and bleomycin, via the PCI mechanism, in a variety of *in vitro* and *in vivo* models, including glioma cell lines. The purpose of this study was to examine the efficacy of combined treatments consisting of PDT and the chemotherapeutic agent, 5-fluorouracil (5-FU) in a 3-dimensional spheroid model consisting of F98 rat glioma cells. Spheroids were incubated with a photosensitizer (aluminum phthalocyanine disulfonate; $AlPcS_{2a}$) and irradiated with 670 nm laser light. Three different wash protocols (0, 4 and 24 h) were employed to determine whether any observed interactions between PDT and 5-FU could be attributed to the PCI mechanism, or were simply due to different cytotoxic pathways of the two treatment modalities.

Although the combined PDT + 5-FU treatments resulted in greater suppression of spheroid growth compared to either treatment alone, no statistically significant differences in growth effects were observed between 0 and 4 h wash protocols suggesting that the combined treatment effects were due to different mechanisms of cytotoxicity, rather than a PCI effect.

iii

ACKNOWLEDGEMENTS

To begin, I express my complete appreciation to my thesis advisor, Dr. Steen Madsen, for his assistance and knowledge in the development and understanding of the fields of study involved my research project.

I also express gratitude to Kevin Ashi and Charles Bynum for their time and help in the lab with various aspects regarding my project. I am also very grateful for the assistance of Stephanie Molina, who taught me lab protocols and provided support with other topics. I also like to thank my family for their strength throughout my entire studies.

Lastly, I want to thank Heena Kumar and Gregory Sobczyk for the valuable advice and encouragement throughout my master's studies and thesis project.

TABLE OF CONTENTS

LIST OF TABLES

LIST OF FIGURES

INTRODUCTION

1.1 Glioblastoma Multiforme

High-grade brain tumors such as glioblastoma multiforme (GBM) originate from glial cells located in the central nervous system (CNS). CNS tumors are relatively rare accounting for only about 2% of all cancer deaths (Chandana et al. 2008). GBM is the most common type of glioma accounting for approximately 50% of all gliomas and 15.6% of all primary brain tumors (Table 1). Due to their aggressive and infiltrative nature, GBMs are one of the most deadly types of cancer with one and five-year survival rates of 35% and 4.7%, respectively (Table 2). A variety of GBM subgroups exist but the most aggressive is also the most commonly seen in humans (Holland 2000). Due to the poor prognosis and limited efficacy of current treatments, significant efforts have been devoted to develop alternative treatments including the use of hybrid viruses, gene therapy and a wide variety of immunotherapeutic approaches (Holland 2000). GBMs pose significant therapeutic challenges due to a number of factors including their heterogeneity (multiforme) and invasive behavior. The tumors consist of both rapidly propagating cells as well as regions of necrosis. Numerous genetic alterations are associated with GBM including mutations in the epidermal growth factor receptor (EGFR) and phosphatase and tensin homolog (PTEN) (Alifieris and Trafalis 2015). The collective effect of these mutations is to disrupt the cell cycle resulting in uncontrollable cell division.

The primary treatment for GBM is surgical resection with the aim of removing as much of the tumor as possible. Unfortunately, due to the infiltration of glioma cells into normal brain, surgery is not sufficient to eradicate the disease. A complicating factor for achieving complete resection is the inability to visualize infiltrating glioma cells with current imaging modalities such as magnetic resonance imaging. Secondary treatments involving radiation and chemotherapy are typically used in an attempt to eradicate infiltrating glioma cells however, as evidenced from high recurrence

1

rates, these treatments are ineffective thus providing the rationale for alternative localized treatment approaches, including light-based techniques such as photochemical internalization (PCI) aimed at eliminating infiltrating cells in normal brain.

Histology	Total			
	N	% of All Tumors	Median Age	Rate
Tumors of Neuroepithelial Tissue	**101,825**	**31.2**	**56**	**6.60**
Pilocytic astrocytoma	4,741	1.5	13	0.33
Diffuse astrocytoma	8,535	2.6	47	0.56
Anaplastic astrocytoma	5,621	1.7	54	0.37
Glioblastoma	50,872	15.6	64	3.19
Oligodendroglioma	4,020	1.2	43	0.27
Ependymal tumors	6,304	1.9	44	0.42
Glioma malignant, NOS	6,765	2.1	38	0.46
Neuronal and mixed neuronal-glial tumors	4,036	1.2	27	0.27
Embryonal tumors	3,790	1.2	9	0.26
Tumors of Cranial and Spinal Nerves	**26,564**	**8.1**	**55**	**1.69**
Nerve sheath tumors	26,548	8.1	55	1.69
Tumors of Meninges	**121,110**	**37.1**	**65**	**7.71**
Meningioma	116,986	35.8	65	7.44
Lymphomas and Hemopoietic Neoplasms	**7,122**	**2.2**	**65**	**0.46**
Lymphoma	6,919	2.1	65	0.44
Germ Cell Tumors and Cysts	**1,464**	**0.4**	**17**	**0.10**
Tumors of Sellar Region	**50,709**	**15.5**	**50**	**3.32**
Tumors of the pituitary	47,958	14.7	51	3.13
Unclassified Tumors	**17,917**	**5.5**	**64**	**1.16**
Hemangioma	3,934	1.2	49	0.26
Neoplasm, unspecified	13,895	4.3	70	0.90
TOTAL‡	**326,711**	**100**	**59**	**21.03**

Table 1 Incidence rates of CNS tumors. Rates are per 100,000 and are age-adjusted to the 2000 U.S. standard population (Ostrom et al. 2013).

2

Histology	N	1-Yr	5-Yr
		%	%
Pilocytic astrocytoma	3,301	97.9	94.4
Diffuse astrocytoma	5,902	71.3	47.3
Anaplastic astrocytoma	3,472	60.1	26.5
Glioblastoma	28,212	35.0	4.7
Oligodendroglioma	3,226	93.8	79.1
Anaplastic oligodendroglioma	1,257	80.6	50.7
Ependymal tumors	2,517	93.9	83.4
Oligoastrocytic tumors	1,820	87.2	61.0
Glioma malignant, NOS	4,014	61.1	43.4
Neuronal and mixed neuronal-glial tumors	469	90.2	74.5
Embryonal tumors	2,666	81.5	61.3
Medulloblastoma	1,573	88.2	71.1
Primative neuroectodermal tumor	651	76.4	49.5
Atypical teratoid/rhabdoid tumor	181	48.1	28.0
Other embryonal histologies	261	76.3	54.2
Meningioma	1,099	82.6	64.7
Lymphoma	4,500	47.6	29.1
Total: All Brain and Other Nervous System	**66,830**	**56.9**	**33.8**

Table 2 One- and five-year relative survival rates for selected malignant brain and central nervous system tumors by histology (Ostrom et al. 2013).

1.2 Photodynamic Therapy

PDT is the use of light and a photosensitizer to cause cell damage (Figure 1). Following photosensitizer administration, light of a particular wavelength matching an absorption resonance of the photosensitizer, is used to excite the molecule. The excited photosensitizer interacts with ground state molecular oxygen resulting in the generation of singlet molecular oxygen, a potent reactive oxygen species, resulting in cell death (Figure 2) (Robertson, Evans, and Abrahamse 2009). Like radiation therapy, PDT is an oxygen-mediated treatment and, as such, efficacy is sensitively dependent on the presence of oxygen during treatment.

3
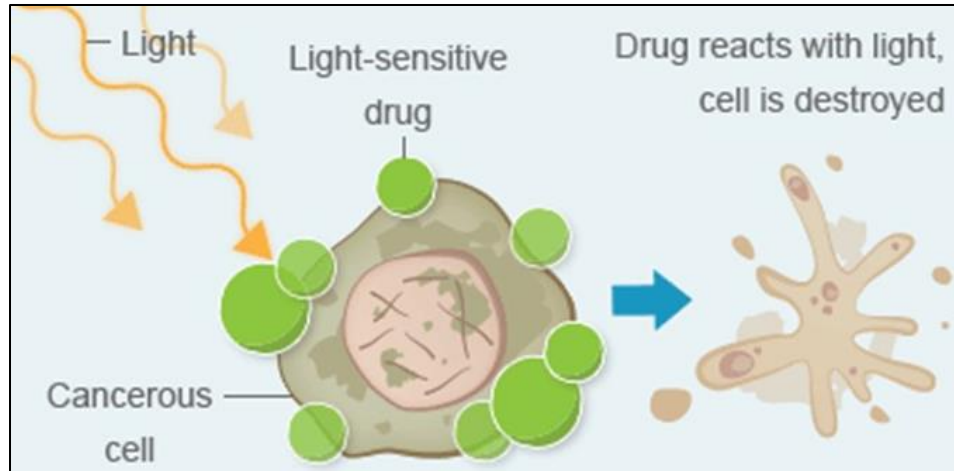
Figure 1 Overview of PDT (Godfrey 2018)

PDT is somewhat limited by the poor penetration depth of light in biological tissues (typically a few mm) and therefore light must be delivered in close proximity to the tumor. This is typically accomplished using laser light coupled into optical fibers in contact with or embedded into the tumor and, as such, this approach provides a high degree of tumor selectivity which is important since most photosensitizers have rather poor specificity (Robertson, Evans, and Abrahamse 2009). PDT efficacy depends on a number of factors including photosensitizer type, light dose and dose rate, and tissue oxygenation status.
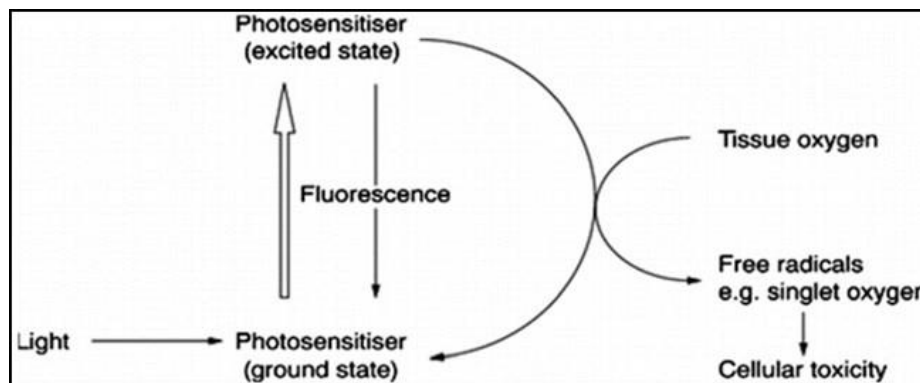
Figure 2 PDT toxicity via generation of oxygen radicals (Joy et al. 2014) .

Photosensitizers with strong absorption in the red to near-infrared are desirable since light has optimum penetration in biological tissues in this wavelength range. This optical window is due to the limited absorption of tissue chromophores in the red to near-infrared region of the

4

electromagnetic spectrum (Chester, Martellucci, and Scheggi 1991). Light delivered at low dose rates has been found to be more effective compared to high dose rate PDT in a number of *in vitro* and *in vivo* models and hence, provides the rationale for the low dose rate used in this work (Madsen et al. 2006). High dose rates have been shown to result in photobleaching of the sensitizer thus rendering it incapable of producing singlet oxygen – the primary cytotoxic species in PDT. From a mechanistic standpoint, PDT has been shown to affect various levels of cell signaling, e.g. it can increase the levels of intracellular calcium in cancer cells as well as the level of ceramide, a potent inducer of apoptotic cell death. PDT has also been shown to disrupt the epidermal growth factor receptor (EGFR) which is known to help tumors proliferate. Transcription factors are also affected as well as cytokines, which are proteins that control immune responses and other related functions (Robertson, Evans, and Abrahamse 2009).
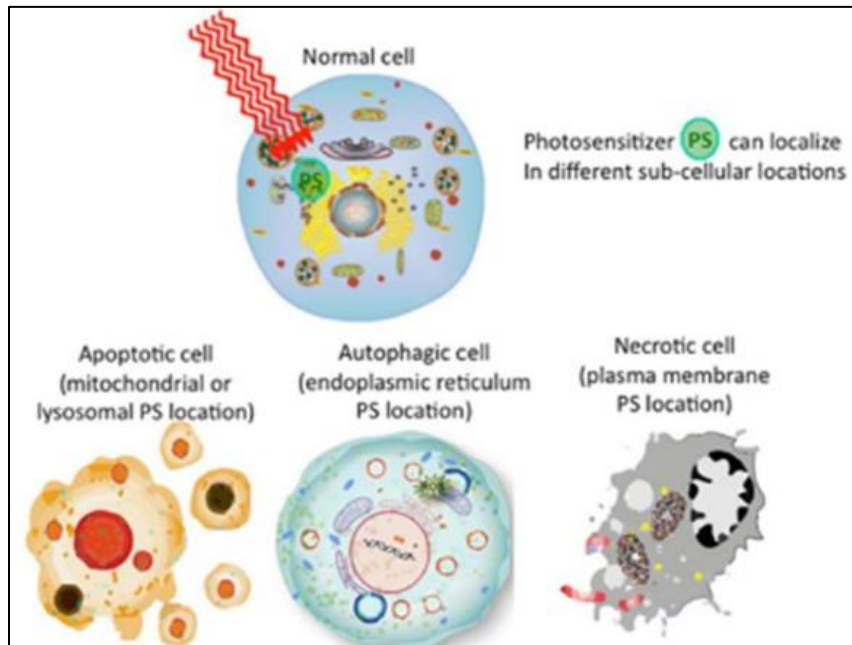

Figure 3 PDT-induced types of cell death (Abrahamse and Hamblin 2016).

PDT can induce either apoptosis, autophagy or necrosis depending on a number of factors including type of photosensitizer, light dose and dose rate (Figure 3). Unlike ionizing radiation

and many chemotherapeutic agents, PDT does not exert its effects via DNA damage (Robertson, Evans, and Abrahamse 2009).

1.3 The use of PDT for the treatment of brain tumors

PDT has been investigated as an adjuvant for the treatment of malignant gliomas for approximately 35 years (Quirk et al. 2015). Although numerous clinical trials have been initiated, the vast majority have consisted of uncontrolled phase I/II studies. Due to differences in methodology and types of malignant brain tumors treated, it has been very difficult to evaluate PDT efficacy from these limited trials. In order for PDT to gain widespread clinical acceptance, it must demonstrate outcomes similar to, and hopefully better, than those achievable with the current standard of care consisting of surgical resection + radiation + temozolomide which results in a median overall survival of 14.6 months and median progression free survival of 6.9 months for newly diagnosed GBM (Stupp et al. 2005).

In a large phase I/II clinical trial conducted in Melbourne, newly diagnosed GBM patients were treated with high light dose PDT (240 J cm^{-2}) using a first generation photosensitizer (Stylli et al. 2005). Mean overall survival (14.3 months) compared favorably with the current standard of care. The results of a clinical trial involving 112 patients with newly diagnosed GBM in Toronto were rather disappointing (mean overall survival of 7.6 months)(Muller and Wilson 2006). The modest results were likely due to the low light dose used (58 J cm^{-2}). Additional trials involving both newly diagnosed and recurrent GBM patients in Munich (Beck et al. 2007), Innsbruck (Beck et al. 2007) and Dundee (Eljamel, Goodman, and Moseley 2008) have failed to show substantial improvements in both overall survival and progression free survival compared to the standard of care. Results of two recent small scale PDT trials in Japan were rather encouraging (Akimoto, Haraoka, and Aizawa 2012; Muragaki et al. 2013) as they demonstrated significant improvement

6

in both overall survival and progression free survival in newly diagnosed and recurrent GBMs. The same approach, consisting of a new generation photosensitizer (talaporfin sodium) in combination with spot irradiation of the resection margins, was used in both trials.

Overall, the results of PDT trials for malignant gliomas have been relatively modest thus providing the rationale for alternative treatment approaches such as PCI.

1.4 Photochemical Internalization

Photochemical Internalization (PCI) is a modified form of PDT which has been used to enhance the uptake of a wide variety of macromolecules including proteins, genes, oligonucleotides and chemotherapeutic agents such as bleomycin (Table 3). The PCI process is illustrated in Figure 4. As shown in panel A, many macromolecules enter cells via endocytosis, which results in their encapsulation in endosomes.

Figure 4 The PCI process (Moses and You 2013).
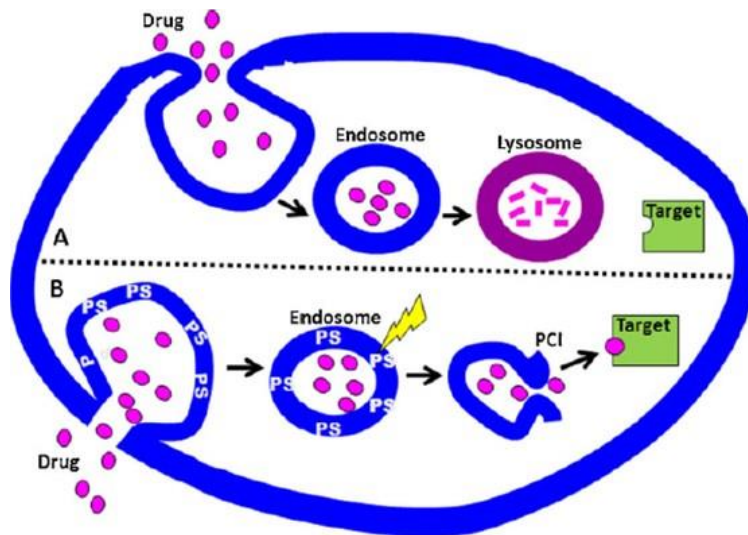
In order to exert their therapeutic effect, macromolecules must be released from the endosomes into the cytosol where they can diffuse to the target (typically the DNA). Unfortunately, only a small fraction of macromolecules escape the endosomes prior to endosome-lysosome fusion which results in the degradation of the macromolecule thus rendering them ineffective. In PCI (panel B),

7

a membrane localizing photosensitizer is administered prior to administration of the therapeutic macromolecule. Following endocytosis, the photosensitizer laden endosome walls are exposed to light and the resultant PDT effect ruptures the membranes thus releasing the macromolecules into the cytosol prior to endosome-lysosome fusion, this process is known as the "light after" approach (Weyergang et al. 2011).

Cancer type	In vivo/In vitro	Photosensitizer	Cytotoxic agents	References
Uterus cancer	In vitro	$TPPS_4$, $TPPS_{2a}$ $AlPcS_{2a}$, $TPCS_{2a}$	Doxorubicin, Gelonin Cetuximab-Saporin	(Pål Kristian Selbo, Sandvig, et al. 2000) (Olsen et al. 2013) (Wai et al. 2007)
Head and Neck cancer	In vitro	tetraphenyl porphine $AlPcS_{2a}$ TPPS2a	Ranpirnase Saporin PAMAM-saporin	(Liebers et al. 2017) (Lai et al. 2008) (Wang et al. 2012)
Breast cancer	In vitro	$TPPS_{2a}$, $TPCS_{2a}$ $AlPcS_{2a}$	EGF-saporin, Doxorubicin Gelonin, IM7-saporin	(Pål Kristian Selbo et al. 2012) (Olsen et al. 2013) (Bostad et al. 2014)
	In vivo	DPc, $TPCS_{2a}$	(DPc/m) Doxorubicin scFvMEL-rGel	(Lu et al. 2011) (Eng et al. 2018)
Colon cancer	In vitro	$TPPS_{2a}$ $AlPcS_{2a}$ $TPCS_{2a}$	MOC31-gelonin, Trastuzumab–saporin Cetuximab–saporin	(Pål Kristian Selbo, Sivam, et al. 2000) (Berstad, Weyergang, and Berg 2012) (Wai et al. 2007)
	In vivo	$AlPcS_{2a}$	Bleomycin Gelonin	(Pl Kristian Selbo et al. 2001) (Pl Kristian Selbo et al. 2001)
Ovarian cancer	In vitro	$TPPS_{2a}$	EGF–saporin (liposomally encapsulated saporin)	(Weyergang, Selbo, and Berg 2006) (Fretz et al. 2007)
Sarcoma	In vitro	$TPCS_{2a}$, $AlPcS_{2a}$ $TPPS_{2a}$	IM7-saporin Gelonin	(Bostad et al. 2014) (Dietze et al. 2003)
	In vivo	$AlPcS_{2a}$	Bleomycin Gelonin	(O.-J. Norum, Giercksky, and Berg 2009) (Berg et al. 2005)
Bladder cancer	In vitro	$TPCS_{2a}$ $TPPS_{2a}$, $AlPcS_{2a}$	Bleomycin scFvMEL/rGel	(Arentsen et al. 2014) (Pål K. Selbo et al. 2009)
	In vivo	$TPCS_{2a}$	Bleomycin	(Gederaas et al. 2017)
Glioma	In vitro	$AlPcS_{2a}$	Doxorubicin Bleomycin	(Shin et al. 2018) (Mathews et al. 2012)
	In vivo	$AlPcS_{2a}$	Bleomycin, ETXp	(Hirschberg et al. 2009)
Skin cancer	In vitro	$TPPS_{2a}$ $AlPcS_{2a}$	Cetuximab–saporin Gelonin	(Wai et al. 2007) (Prasmickaite et al. 2002)
	In vivo	$AlPcS_{2a}$, $TPPS_{2a}$	scFvMEL/rGel	(Pål K. Selbo et al. 2009)
Prostate cancer	In vitro	$TPPS_{2a}$	cetuximab–saporin IM7-saporin	(Wai et al. 2007) (Bostad et al. 2014)
Pancreatic cancer	In vitro	$TPCS_{2a}$	IM7-saporin anti-CD133	(Bostad et al. 2014) (Bostad et al. 2013)
Lung cancer	In vitro	$AlPcS_{2a}$, 3-THPP[2]	MOC31-gelonin	(Pål Kristian Selbo, Sivam, et al. 2000)

Table 3 Summary of macromolecules used in PCI.

8

1.5 Cell line

F98 rat glioma cells were used in this study (Figure 5). The cells were originally derived from transformed fetal Fischer rat brain cells following exposure to a known carcinogen (ethyl-nitrosourea) (Ko, Koestner, and Wechsler 1980). The F98 cell line has been used in a number of *in vitro* and *in vivo* studies evaluating the effects of a variety of therapeutic modalities including PDT (Madsen, Kharkhuu, and Hirschberg 2007). The cell line shares many characteristics with human GBM including infiltrative behavior and rapid proliferation. Furthermore, when F98 cells are implanted into brains of Fischer rats, tumors develop rapidly and are highly reproducible from animal to animal. The weak immunogenicity of F98 tumors is a substantial advantage over other rat glioma cell lines which have been shown to evoke strong immune responses (Barth and Kaur 2009).
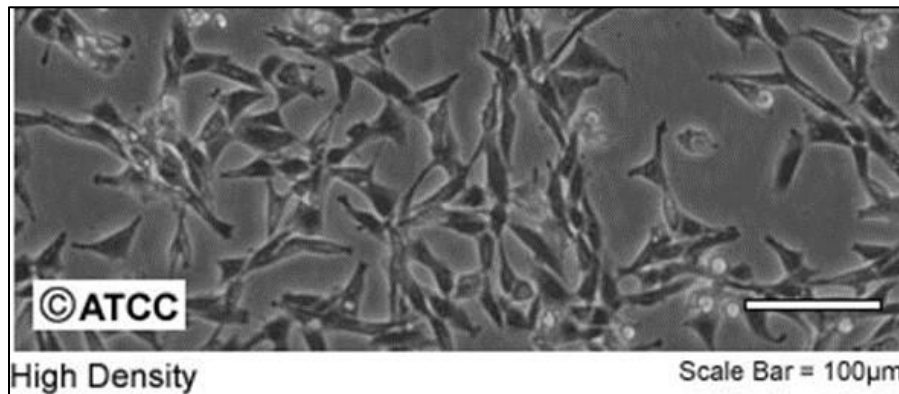
Figure 5 F98 rat glioma cells (ATCC 2016).

1.6 Spheroids

The majority of *in vitro* therapeutic studies have been conducted on cells arranged in monolayers since this is an easy model to maintain. In this configuration, all cells have adequate access to nutrients and oxygen in the cell medium. Unfortunately, monolayers do not mimic the three-dimensional nature of solid tumors and the resultant nutrient and oxygen gradients affect therapeutic response, especially for oxygen-mediated therapies such as ionizing radiation and

9

PDT. Spheroids are three-dimensional cell clusters that closely resemble the tumor environment (Santini, Rainaldi, and Indovina 2000). Of particular relevance to this work is the ability of multicellular spheroids to mimic the oxygen gradients found in tumors. As shown in Figure 6, as spheroids grow beyond a diameter of 250 - 300 µm diameter, a central core of necrosis develops due to the limited diffusion of oxygen from its source (Dubessy et al. 2000).
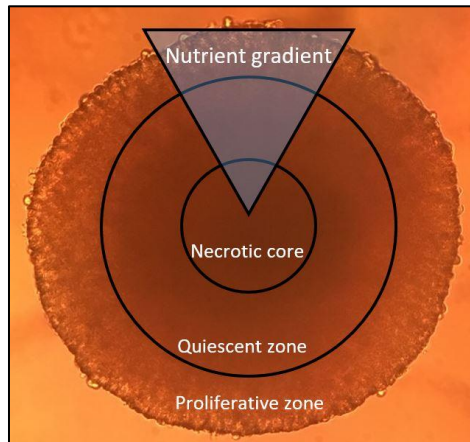
Figure 6 Three-dimensional spheroid consisting of F98 cells illustrating the characteristic cell viability zones, modified from (LaBonia et al. 2016)

Although cells in the necrotic core are dead and therefore not of relevance in therapeutic studies, cells adjacent to the necrotic core are hypoxic and therefore resistant to PDT. Due to the lack of oxygen, these cells are not proliferating and are therefore found in the quiescent (G_0) stage of the cell cycle. As in solid tumors, these resistant cells are treatment limiting. The outermost layer of cells in the spheroid are in a relatively oxygen rich environment as they are closest to the source of oxygen, i.e., the medium and therefore they proliferate rapidly. In addition to the oxygen gradients, spheroids are also capable of mimicking photosensitizer gradients found in tumors including the effects of the extracellular matrix which may impede diffusion of the sensitizer. Since spheroid diameters were approximately 250 – 300 µm at the time of laser irradiation, light distributions were relatively uniform throughout the spheroid.

Although the lack of a vasculature is a drawback of the spheroid model it may be possible to address this limitation by placing spheroids on the surface of the developing chick embryo. For example, De Magalhães et al. 2010 found significant vascularization of human glioma spheroids 7 days following implantation on the chick chorioallantoic membrane.

1.7 5-Fluorouracil

A number of chemotherapeutic agents have been used in the treatment of GBM. Ideally these drugs should have the ability to cross the blood-brain barrier followed by entry into cells through the plasma membrane. This typically occurs only for low molecular weight and/or lipophilic drugs via passive diffusion across the cell membrane (Mathews et al. 2012). Unfortunately, many chemotherapeutic drugs are large and hydrophilic thus requiring active transport into cells via endocytosis (Zaniboni, Prabhu, and Audisio 2005). As discussed previously, PCI may be used to enhance the efficacy of these macromolecules. In the majority of studies reported to date, PCI has been used to enhance the efficacy of bleomycin – a 1.5 kDa glycopeptide antibiotic that causes single and double strand DNA breaks similar to the damage caused by ionizing radiation. PCI has been shown to enhance the efficacy of bleomycin in a number of different cell lines including gliomas (Madsen et al. 2009). 5-Flurouracil (5-FU) is an antimetabolite (Figure 7) that has received FDA approval for the treatment of a wide variety of cancers including colon, rectal, breast, head and neck, cervical and a number of gastrointestinal tumors.(Longley, Harkin, and Johnston 2003). 5-FU acts primarily as a thymidylate inhibitor. Inhibition of this enzyme blocks synthesis of pyrimidine thymidine which is required for DNA replication. Ultimately, administration of 5-FU results in preferential death of rapidly dividing cancer cells. Other mechanisms of action include the downregulation of various RNA processes and activation of the tumor suppressor gene, p53 resulting in apoptotic cell death.(Longley, Harkin, and Johnston 2003). 5-FU is a small molecule

11

(130 Da) that enters the cytoplasm via passive diffusion. Nevertheless, a recent study has shown that PDT and 5-FU interact in a synergistic manner akin to that observed with PCI (Christie et al. 2017).
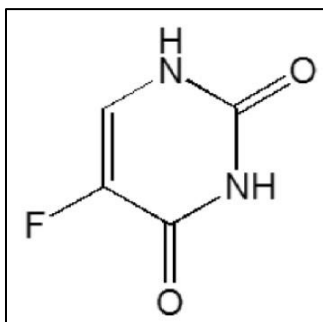
Figure 7 Molecular structure of 5-FU (He et al. 2015).

1.8 Photosensitizer

The photosensitizer used in this work, $AlPcS_{2a}$, is a phthalocyanine derivative containing two charged sulfonate groups linked to phthalic subunits in adjacent positions and an aluminum metal ion incorporated at its center (Figure 8). Of particular relevance to PCI is that $AlPcS_{2a}$ is an amphiphilic molecule, i.e., it has both hydrophilic and lipophilic properties and therefore it localizes in cellular membranes following systemic administration (Hirschberg and Madsen 2017). The lipophilic phthalocyanine skeleton of $AlPcS_{2a}$ localizes in the lipophilic interior of the cellular membrane while the sulfonate groups dissolve in the hydrophilic outer layer of the membrane.
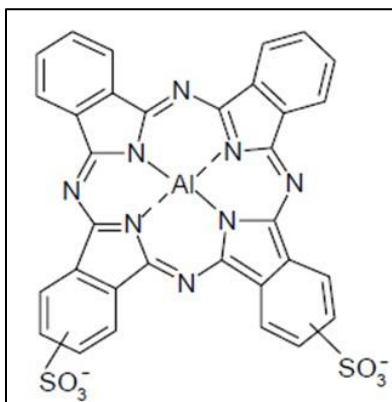
Figure 8 Molecular structure of AlPcS2a (Pål Kristian Selbo et al. 2002).

12

1.9 Scope of Work

The purpose of this work was to determine the efficacy of combined 5-FU and $AlPcS_{2a}$-PDT in an *in vitro* model consisting of three-dimensional multicell F98 glioma spheroids. Specifically, different wash protocols were investigated to determine whether any observed interaction between the two treatments could be attributed to the PCI mechanism, or was simply due to different cytotoxic pathways of the two modalities.

2.1 Maintenance of Cell Line

All experiments were done at the University of Nevada, Las Vegas. The F98 rat glioma cell line used in this experiment was propagated in T-25 BD Falcon flasks with a vented cap and the media used was Dulbecco's Modified Eagle Medium (DMEM, Thermo Fisher Corp., Carlsbad CA) modified with 15 ml of HEPES, 5 ml of Pen-Strep (10,000 units/ml Penicillin, 10,000 µg/ml Streptomycin, Thermo Fisher Corp., Carlsbad CA) and 50 ml of fetal bovine serum (FBS; Thermo Fisher Corp., Carlsbad CA). Cells were kept in an incubator at the following settings: 37°C, 5% CO_2, 80% humidity. The protocol to culture the cells was as follows: at cell confluence, the medium was removed and the adherent F98 monolayer was washed using 5-7 ml of phosphate buffer solution (PBS; Thermo Fisher Corp, Carlsbad CA). Following PBS removal, the monolayer was treated with 5 ml of Gibco Trypsin-EDTA for five minutes. The detached cells were then used to make spheroids.

2.2 Creation of Spheroids

Following cell detachment, PBS (7-10 ml) was added to the cells and the resultant solution was transferred to a 15 ml centrifuge tube which was placed into a centrifuge and spun at a setting of 400 g for 4 minutes. Following centrifugation, the cells formed a pellet at the bottom of the tube. The excess PBS was removed, replaced with fresh PBS and vortexed. This process was then repeated. Media was then added instead of PBS followed by vortexing to disperse the pellet. Cells were counted using a C-Chip (SKC Inc., Covington CA). The spheroids were generated using a total of 12000 cells per ml. The cells in 100 µl of medium were alloquated into individual wells of a Costar 96 well round bottom ultra-low attachment plate (Fisher Scientific, Inc., Pittsburgh PA), centrifuged at 400 g for 4 min. and placed in an incubator for 45-60 min. Following incubation, the plate was then centrifuged a second time at 800 g for 8 min. Cells in each well were visually

14

inspected using a microscope to confirm a disc shaped appearance. The plate was placed in the incubator (37°C, 5% CO_2, 80% humidity) for 48 h to allow the spheroids to assume their characteristic 3-D shape. In the case of the PCI experiments, five plates were centrifuged: dark controls, PDT controls, and 3 PCI experimental plates. In all cases, the mean spheroid diameter prior to the initiation of treatment was 250 – 300 µm.

2.3 5-FU Procedure

Five mg/ml of 5-FU in DMSO was diluted to a 1 mg/ml stock solution with PBS. The stock solution was then diluted with DMEM to the following concentrations: 0.25, 0.5 and 1 µg/ml. Controls (0 µg/ml) consisted of spheroids in DMEM only. Two days following creation, spheroids were incubated in various 5-FU concentrations. Each well consisted of 200 µl 5-FU-DMEM solution (or DMEM in the case of controls) which was replaced with new medium 5 days following incubation and, as such, spheroids were incubated with various concentrations of 5-FU for 5 days.

2.4 Laser Setup

The setup for laser irradiation is shown in Figure 9. Spheroids were irradiated with a 670 nm diode laser (Intense, North Brunswick NJ) coupled to a 200 µm dia. optical fiber (Medlight SA, Ecublens, Switzerland). A ring stand was used in combination with a cardboard cutout which allowed the plates to be elevated above the laser thus facilitating spheroid irradiation from the bottom of the plate. The cardboard cutout ensured irradiation of only three columns at a time. In all cases, spheroids were irradiated with a 9 cm dia. beam at an irradiance of 5 mW/cm^2 for 60, 120, or 200 s corresponding to radiant exposures of 0.3, 0.6, or 1.0 J cm^{-2}, respectively. On a given plate, each irradiated group was separated by two empty columns in order to minimize the effects of light scattering and its contribution to light dose to spheroids in the other radiant exposure groups.

15
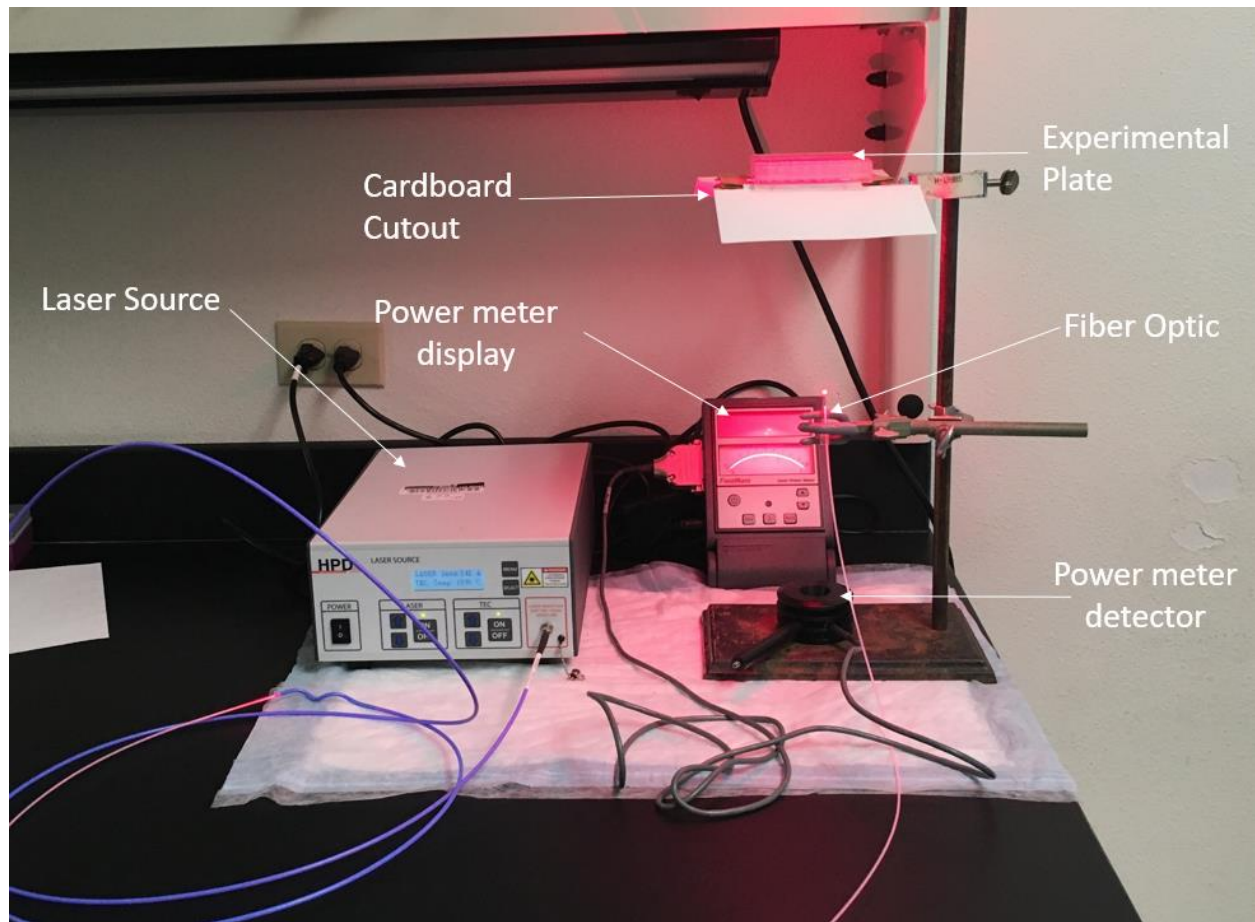
Figure 9 Experimental setup showing laser irradiation of 96-well plate.

2.5 Photodynamic Therapy Procedure

Forty-eight hours following centrifugation, spheroids were examined with a light microscope to ensure their characteristic 3D shape prior to PDT treatments. The photosensitizer $AlPcS_{2a}$ (Frontier Scientific, Inc., Logan UT) was diluted to a concentration of 2 µg/ml with DMEM and 100 µL of this solution was added to each spheroid in the 96 well plate (one spheroid per well). The plate was covered with aluminum foil to minimize background light exposure and placed in an incubator for 18 h. Following incubation, the photosensitizer was removed from each well using a wash protocol consisting of replacing the photosensitizer solution with 100 µl PBS. A total of four washes were performed to ensure complete removal of the sensitizer. The spheroids were then irradiated either immediately following the wash cycle (0 h protocol), 4 h later (4 h protocol), or

16

24 h later (24 h protocol) according to the light protocols described in section 2.4. Following PDT treatments, the plates were placed in an incubator for 48 h after which the first spheroid volumes were recorded. All procedures described in this section were performed under subdued light conditions in order to minimize the possibility of ambient light-induced PDT toxicity.

2.6 Combined PDT + 5-FU Procedure

Except for the addition of 5-FU, the combined treatment protocol was identical to the PDT procedure described in Section 2.5. 5-FU was diluted with DMEM to a concentration of 0.25 µg/ml and 100 ul of this solution was added to each well containing a PDT + 5-FU-designated spheroid. In the case of the 0 h protocol, spheroids were irradiated immediately following the addition of 5-FU. For the four hour protocol, spheroids were irradiated 4 h after 5-FU incubation. This is the standard PCI protocol employing bleomycin. In the case of the 24 h protocol, 5-FU was added 24 h after the last wash followed immediately by light irradiation. The three protocols are summarized below.

<div align="center">

0 h Protocol

18 h AlPcS$_{2a}$ incubation → wash → wash → wash → wash --- 5-FU → light

4 h Protocol

18 h AlPcS$_{2a}$ incubation → wash → wash → wash → wash → 5-FU -- 4 h → light

24 h Protocol

18 h AlPcS$_{2a}$ incubation → wash → wash → wash → wash → 24 h → 5-FU ---light

</div>

Following light exposure, the plates were placed in an incubator for 48 h after which the first spheroid volume measurements were made.

17

2.7 Measurements and Analysis

In all cases, treatment efficacy was determined from spheroid growth kinetics. A light microscope with a calibrated eyepiece was used to measure spheroid diameters. For each spheroid, the mean of two diameter measurements (vertical and horizontal) were recorded and the volume calculated assuming a perfect sphere. Spheroids (12 per experimental group) were followed for approximately two weeks. Spheroids were measured 5, 8, 10 and 13 days following treatment and normalized spheroid volume was plotted to determine treatment efficacy. Normalized volume was determined by calculating the ratio of volumes of treated to untreated controls on the last measurement day. In order to determine the degree of interaction between PDT and 5-FU, the following equation was used (Drewinko et al. 1976):

$$\alpha = \frac{V^{PDT} * V^{5-FU}}{V^{PDT+5-FU}}$$

where V^{PDT}, V^{5-FU} and $V^{PDT+5-FU}$ represent normalized volumes of spheroids subjected to PDT, 5-FU and PDT + 5-FU. In this scheme, an alpha value of one represents an additive effect while alpha values less than or greater than one represent antagonistic or synergistic effects respectively. Student t-tests were performed to determine whether the results of the different wash protocols were statistically significant (www.graphpad.com).

18

3.1 5-FU dose dependence

The effects of 5-FU on F98 spheroids are shown in Figure 10. Normalized spheroid volumes ranged from 0.72 at the lowest 5-FU concentration investigated (0.12 µg/ml), to 0.17 at the highest concentration (0.5 µg/ml). Based on these results, a concentration of 0.12 µg/ml 5-FU was used for all subsequent PCI studies. The rationale for this choice is based on the objective of PCI which is to enhance the effects of therapeutic drugs at relatively low concentrations.
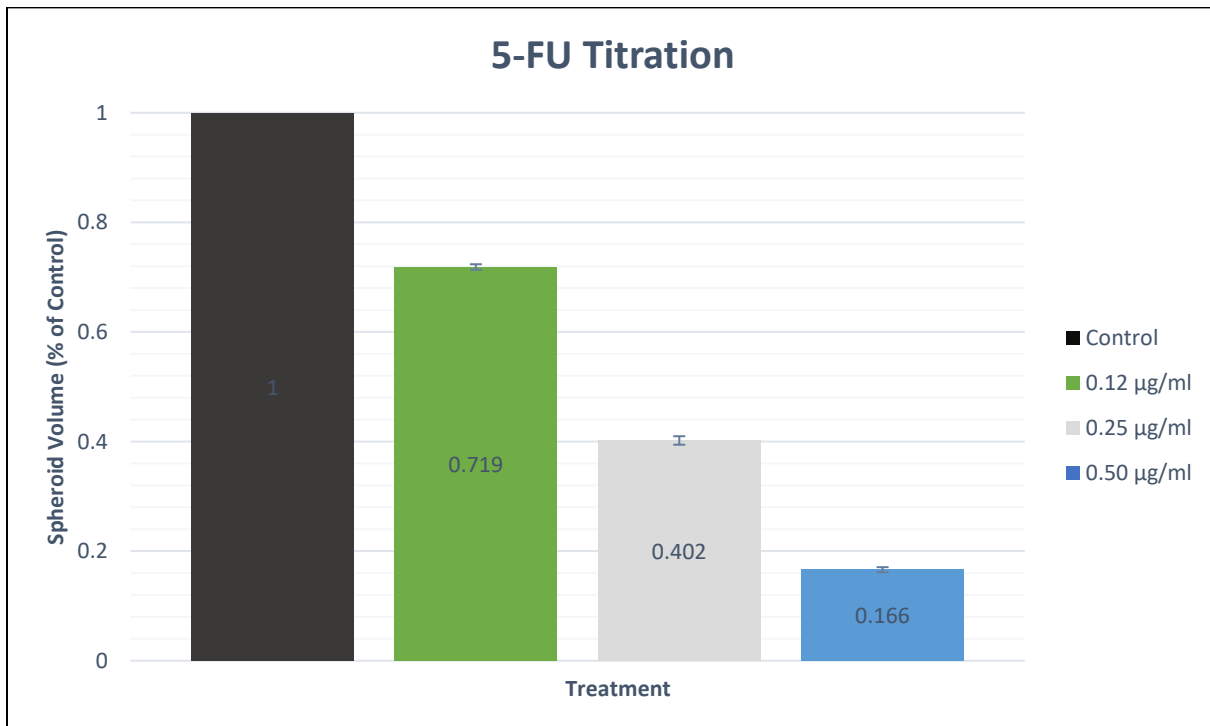
Figure 10 Effects of 5-FU on F98 spheroid growth. Spheroids were incubated in varying concentrations of 5-FU for 5 days. Normalized spheroid volumes were recorded 13 days following the start of incubation. Each data point represents the mean of 6 trials (12 spheroids per trial) and error bars represent standard deviations

3.2 PDT results

The effects of PDT on spheroid growth are illustrated in Figure 11 for three different wash protocols. The purpose of the wash was to remove excess photosensitizer from the wells prior to light irradiation. In standard PDT protocols, spheroids are irradiated immediately following the wash cycle, i.e., the 0 h protocol (Figure 11a). The data in Figure 11a show a moderate PDT dose

response ranging from 0.86 ± 0.06 at a radiant exposure of 0.3 J cm^{-2} to 0.69 ± 0.07 at 1.0 J cm^{-2}. A similar dose response was observed for spheroids subjected to PDT after a 4h wash protocol (Fig. 11b) where normalized volumes ranged from 0.97 ± 0.08 for spheroids exposed to 0.3 J cm^{-2}, to 0.73 ± 0.09 following exposures to 1.0 J cm^{-2}. PDT-treated spheroids subjected to the 24 h wash protocol demonstrated only a marginal response ranging from 1.03 ± 0.04 for 0.3 J cm^{-2} to 0.89 ± 0.04 for a radiant exposure of 1.0 J cm^{-2} (Figure 11c). As evidenced from the student t-tests summarized in Table 4, statistical significance was demonstrated in most cases. Overall, the data suggest that the 0 h wash protocol was the most effective for inhibiting spheroid growth while the 24 h protocol was the least effective.

0 h vs. 4 h		4 h vs. 24 h	
Radiant Exposure (J cm^{-2})	p-value	Radiant Exposure (J cm^{-2})	p-value
0.3	0.024	0.3	0.139
0.6	0.040	0.6	0.004
1.0	0.317	1.0	0.001

$p < 0.05$ is considered statistically significant

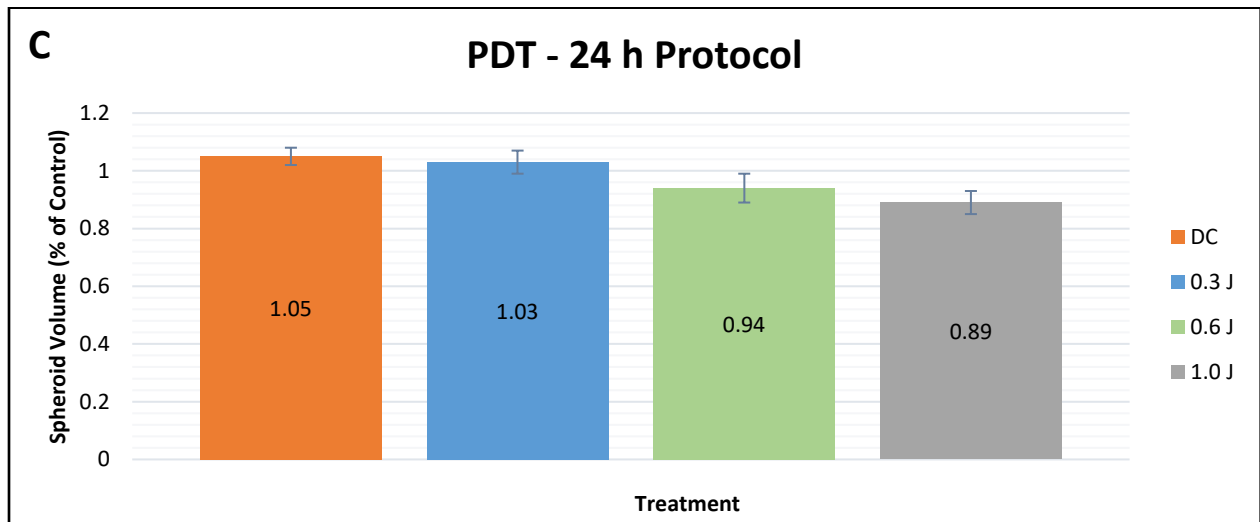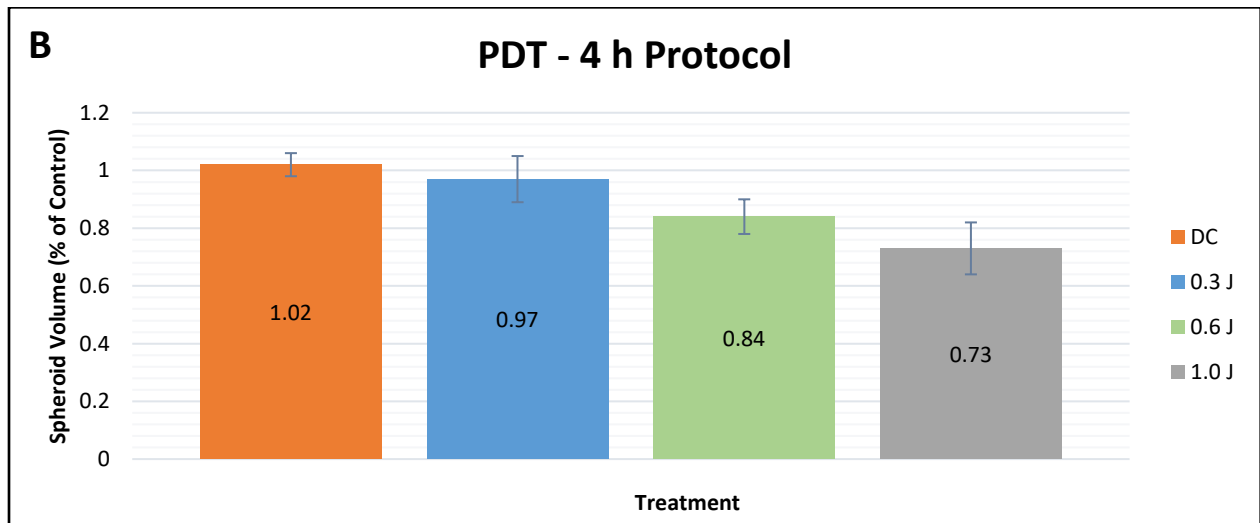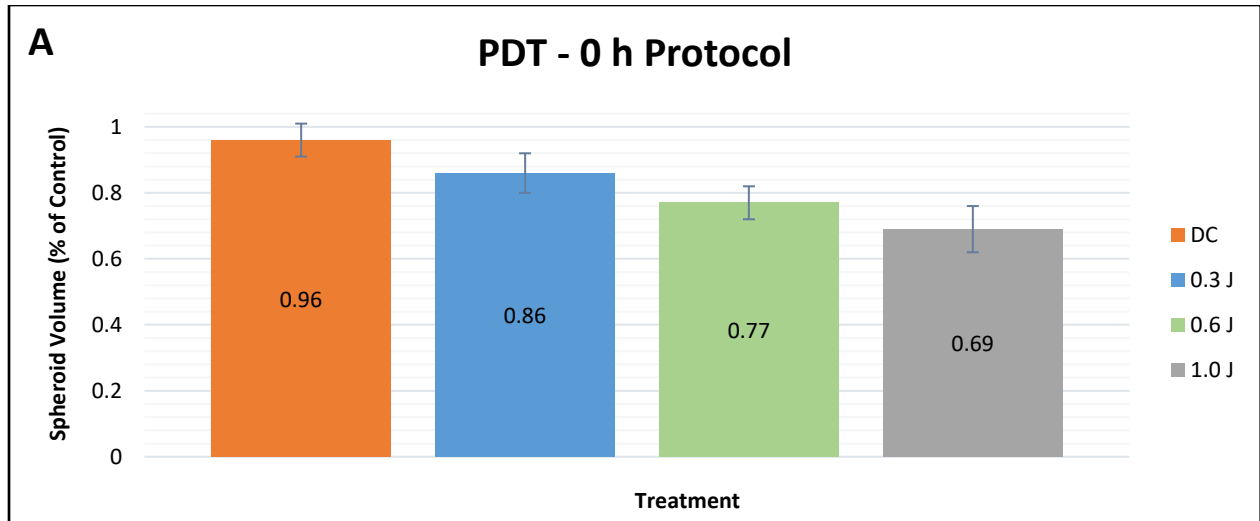Table 4 Evaluation of statistical significance for different wash protocols

20

Figure 11 PDT effects on F98 glioma spheroids subjected to three different wash protocols. Normalized spheroid volumes were recorded 13 days following light exposure. Each data point represents the mean of 6 trials (12 spheroids per trial) and error bars represent standard deviations.

21

3.3 PDT + 5-FU results

Results of the combined experiments are summarized in Figure 12. Significant treatment effects were observed for spheroids subjected to the 0 and 4 h wash protocols. For example, normalized volumes for 0 h spheroids ranged from 0.60 ± 0.04 (0.3 J cm^{-2}) to 0.35 ± 0.04 (1.0 J cm^{-2}) while normalized volumes for the 4 h spheroids ranged from 0.65 ± 0.04 (0.3 J cm^{-2}) to 0.40 ± 0.03 (1.0 J cm^{-2}). In both cases, the greatest effect was observed at the highest radiant exposure. In contrast, treatment efficacy was observed to be lower for 24 h spheroids (Figure 12c) which showed no dependence on radiant exposure (0.68 ± 0.04 for 0.3 J cm^{-2} and 0.64 ± 0.02 for 1.0 J cm^{-2}). In order to obtain a quantitative measure of the degree of interaction between the two treatment modalities, alpha values were calculated from equation (1) and summarized in Table 5. The data show a marginal synergistic effect at the highest radiant exposure for both 0 and 4 h spheroids. In all other cases, $\alpha \sim 1.0$ suggesting an additive effect between PDT and 5-FU.

Radiant Exposure (J cm^{-2})	0 h	4 h	24 h
0.3	1.03 ± 0.10	1.10 ± 0.12	1.11 ± 0.08
0.6	1.18 ± 0.15	1.15 ± 0.14	1.01 ± 0.06
1.0	1.42 ± 0.22	1.35 ± 0.19	1.02 ± 0.06

Table 5 Alpha values for different wash protocols

Spheroid growth kinetics for one trial of each of the three wash protocols are shown in Figure 13 A-C. Not surprisingly, the data show that the PDT + 5-FU protocols result in the greatest growth inhibition. The PDT effect for spheroids subjected to the 24 h wash protocol was marginal compared to the 0 and 4 h spheroids.

22
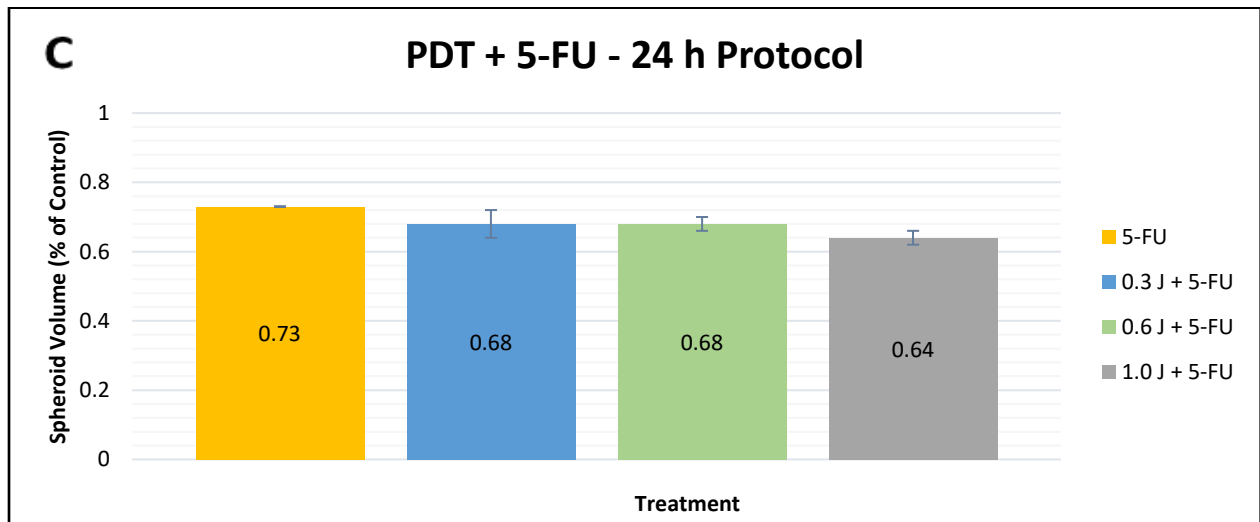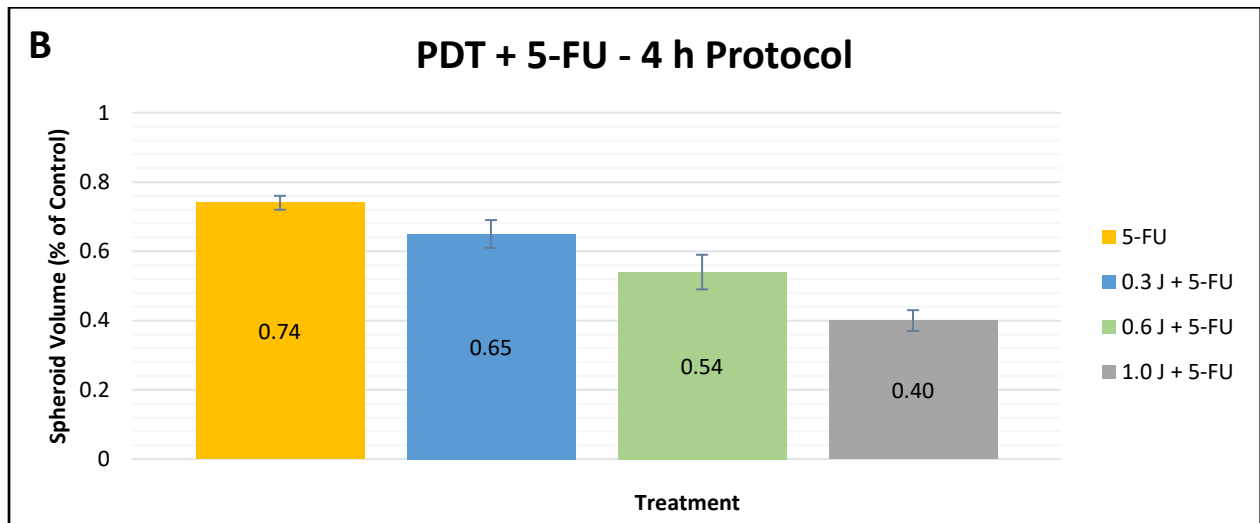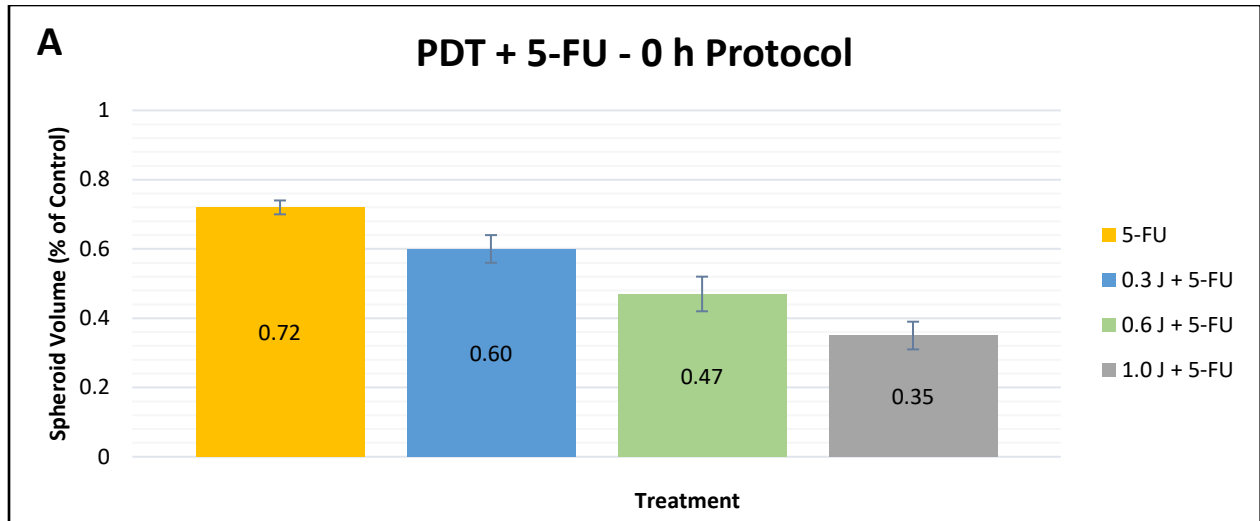
Figure 12 Effects of combined PDT and 5-FU on F98 glioma spheroids subjected to three different wash protocols. Normalized spheroid volumes were recorded 13 days following light exposure. Each data point represents the mean of 4 trials (12 spheroids per trial) and error bars represent standard deviations
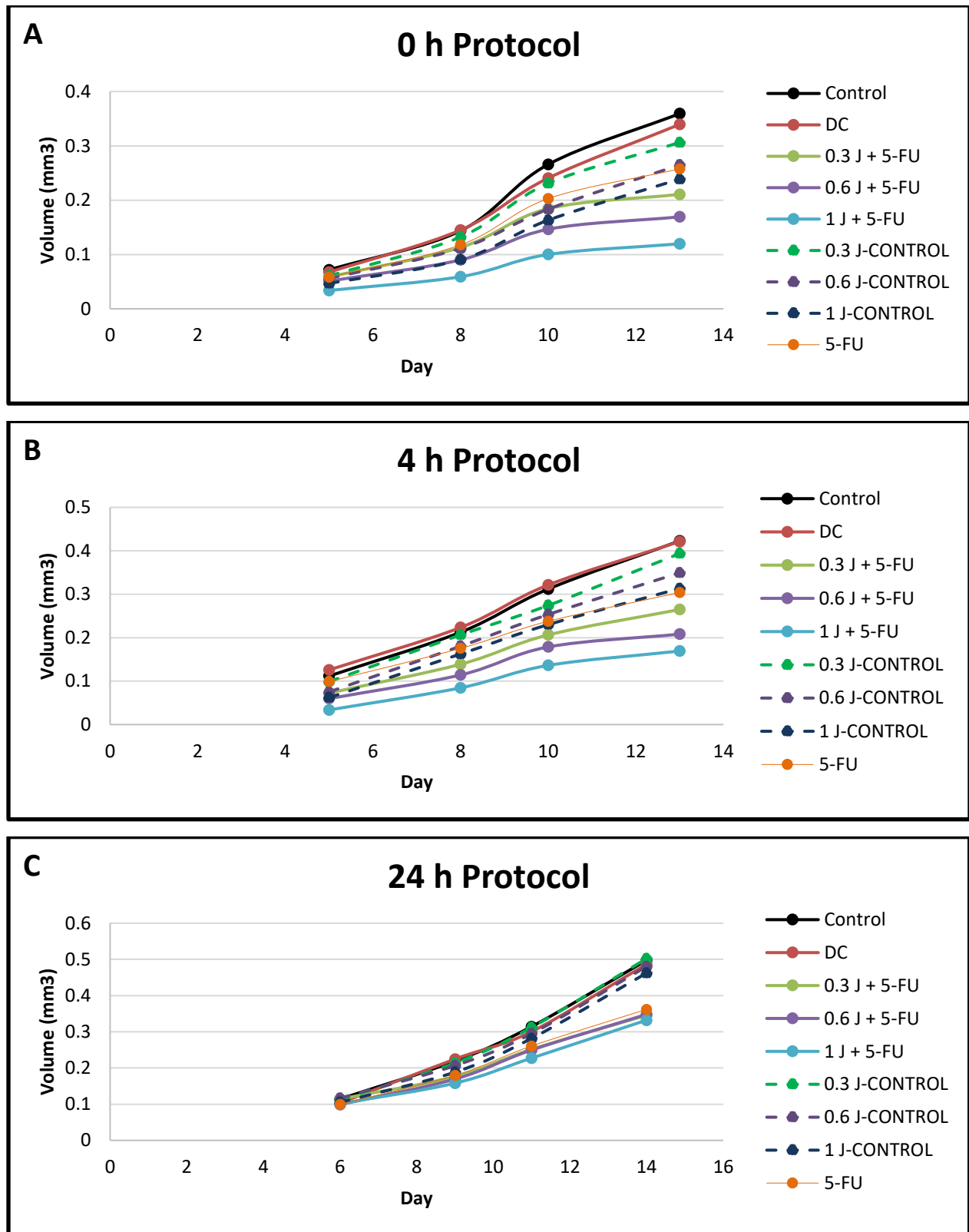
Figure 13 Growth kinetics of F98 glioma spheroids subjected to three different wash protocols. In each case, treatment was initiated on day 0. Each data point represents the mean of 12 spheroids. Standard deviations were too small to plot.

DISCUSSION

PCI is a type of PDT that has been shown to enhance the efficacy of a wide variety of hydrophilic macromolecules with limited ability to cross the cell membrane (Weyergang et al. 2011). PCI has been demonstrated in a wide variety of cell lines and *in vivo* models (Pål Kristian Selbo et al. 2010). Results from the first clinical PCI trial suggest that it may be a useful therapeutic approach for head and neck cancer patients who have failed standard treatments (Sultan et al. 2016). A number of *in vitro* studies employing 3-D multicell glioma spheroids suggest that PCI may be useful for the delivery of large chemotherapeutic drugs, such as bleomycin, to patients with malignant brain tumors (Mathews et al. 2012). Bleomycin is a large hydrophilic molecule that enters the cytosol via endocytosis. In traditional *in vitro* PCI protocols employing bleomycin, cells or spheroids are incubated with a membrane-localizing photosensitizer (e.g. $AlPcS_{2a}$) for 18 h followed by 4 h incubation with bleomycin. The 4 h incubation, allows a sufficient amount of the drug to be internalized in endosomes within the cytosol.

Small lipophilic molecules, such as 5-FU, enter the cytosol via passive diffusion across the plasma membrane and, as such, is not ideally suited for PCI. A recent study showed that PDT enhanced the efficacy of 5-FU in a synergistic manner in F98 spheroids (Christie et al. 2017). The reason for the synergism was unknown, but was likely due to an interaction between PDT and 5-FU, rather than a PCI effect. The thesis experiments, consisting of different wash protocols, were designed to resolve this issue. A true PCI effect between PDT and 5-FU should be manifested by greater spheroid growth inhibition following the 4 h wash protocol. If the 0 and 4 h wash protocols produce similar growth inhibition, a non-PCI interaction between PDT and 5-FU is the likely explanation.

Based on the 5-FU dose response data (Figure 10), the potency of this drug is approximately five times greater than bleomycin. For example, the 5-FU dose required for a 50%

25

reduction in F98 spheroid volume is approximately 0.2 µg/ml. A similar reduction in spheroid volume was observed following a bleomycin dose of approximately 1 µg/ml (Gonzales et al. 2016).

The PDT dose response data (Figure 11) is in good agreement with previous studies employing identical spheroids (Christie et al. 2017). For example, Christie et al. observed normalized spheroid volumes of 85-90% following PDT at a radiant exposure of 0.8 J cm^{-2}. This compares favorably with the normalized volumes observed for the 0 h PDT protocol (77% at 0.6 J cm^{-2} and 69% at 1.0 J cm^{-2}). Overall, the data show that PDT efficacy was greatest when spheroids were irradiated immediately following AlPcS$_{2a}$ incubation (0 h protocol) and least effective if a 24 h interval was inserted following incubation (24 h protocol). This is not surprising since one would expect an increasing amount of photosensitizer to diffuse out of the plasma membrane with time and therefore less AlPcS$_{2a}$ to be available for the PDT effect after 24 h compared to 0 or 4 h.

The combination of PDT and 5-FU produced an enhanced growth effect compared to that observed for either modality alone (Figure 12). Although slight differences in normalized spheroid volumes were observed between 0 and 4 h protocols, none were found to be statistically significant. This suggests that the observed effect was likely not due to PCI. The similar results obtained for the two wash protocols suggest that 5-FU enters the cytosol via passive diffusion rather than by endocytosis which is a requirement for PCI. The calculated alpha values (Table 5) corroborate this conclusion. Based on the alpha values, a synergistic response was observed only for 0 (α = 1.42±0.22) and 4 (1.35±0.19) h spheroids subjected to the highest light exposure. This is a marginal synergistic response compared to previous PCI studies with bleomycin where alpha values are typically in the 2-3 range (Mathews et al. 2012). In all other cases, alpha values were

26

approximately unity suggesting a simple additive effect between PDT and 5-FU. Unlike the 0 and 4 h wash protocols, no light dose dependence was observed for the 24 h spheroids, in fact, normalized volumes for the combined PDT and 5-FU treated spheroids were essentially identical to the 5-FU only treated spheroids suggesting that the observed effect was almost entirely due to 5-FU. This is consistent with the hypothesis that the photosensitizer had leached out of the plasma membrane thus negating the PDT effect.

Overall, the data suggest that there is no PCI effect with 5-FU and therefore the weak synergism observed is likely due to different mechanisms of action of PDT and 5-FU. In contrast to 5-FU, which inhibits RNA transcription and DNA synthesis (Tiraby et al. 1998), $AlPcS_{2a}$-PDT is known to cause damage to the plasma membrane as well as membranes of organelles, such as lysosomes resulting in hydrolase release and cell death via apoptosis (Guicciardi, Leist, and Gores 2004; Kessel, Vicente, and Reiners 2006; Rodriguez et al. 2009) or autophagy (Inguscio, Panzarini, and Dini 2012; Reiners et al. 2010).

CONCLUSIONS

5-FU was found to be a potent cytotoxic agent in the F98 glioma spheroid model and, as such, only very low concentrations were required for the combined studies investigated in this work. The PDT dose response was in good agreement with the findings of other studies using identical spheroids. Not surprisingly, PDT was most efficient following 0 or 4 h wash protocols compared to 24 h protocols. The combination of PDT and 5-FU was more effective than either treatment alone, however, no statistically significant differences were observed between the 0 and 4 h wash protocols suggesting that the observed effects were likely due to different cytotoxic pathways of PDT and 5-FU. Furthermore, the results are consistent with findings that 5-FU enters the cytosol via passive diffusion as opposed to endocytosis which is a requirement for PCI.

Future studies could be performed to elucidate the different mechanisms of $AlPcS_{2a}$-PDT and 5-FU in this cell line. $AlPcS_{2a}$ is a membrane localizing photosensitizer found primarily in the plasma membrane, and to a lesser extent, in membranes of internal organelles such as lysosomes. Therefore, the type of cell death following light irradiation (PDT) is likely dependent on the wash protocol. For example, if spheroids are irradiated immediately following the wash (0 h protocol), necrosis is expected to be the dominant mode of cell death due to damage to the plasma membrane. Some lysosomal damage is also expected, resulting in apoptotic cell death. In contrast, apoptosis is expected to be much more prevalent in spheroids subjected to the 4 h wash protocol since the photosensitizer leaches out of the plasma membrane (while remaining in the lysosome membrane) during the 4 h interval. One would thus expect a shift from necrotic to apoptotic cell death. The mode of PDT-induced cell death in response to different wash protocols could be examined by using commercially available assays for necrosis and apoptosis.

28

REFERENCES

Abrahamse, Heidi, and Michael R Hamblin. 2016. "New Photosensitizers for Photodynamic Therapy." *The Biochemical journal* 473(4): 347–64. http://www.ncbi.nlm.nih.gov/pubmed/26862179.

Akimoto, Jiro, Jo Haraoka, and Katsuo Aizawa. 2012. "Preliminary Clinical Report on Safety and Efficacy of Photodynamic Therapy Using Talaporfin Sodium for Malignant Gliomas." *Photodiagnosis and Photodynamic Therapy* 9(2): 91–99. http://dx.doi.org/10.1016/j.pdpdt.2012.01.001.

Alifieris, Constantinos, and Dimitrios T. Trafalis. 2015. "Glioblastoma Multiforme: Pathogenesis and Treatment." *Pharmacology and Therapeutics* 152: 63–82.

Arentsen, Harm C. et al. 2014. "The Effect of Photochemical Internalization of Bleomycin in the Treatment of Urothelial Carcinoma of the Bladder: An in Vitro Study." *Urologic Oncology: Seminars and Original Investigations* 32(1): 49.e1-49.e6. http://dx.doi.org/10.1016/j.urolonc.2013.07.005.

ATCC. 2016. "F98 EGFR (ATCC® CRL-2948™)." https://www.atcc.org/en/Products/Cells_and_Microorganisms/By_Tissue/Brain/CRL-2948.aspx#characteristics.

Barth, Rolf F., and Balveen Kaur. 2009. "Rat Brain Tumor Models in Experimental Neuro-Oncology: The C6, 9L, T9, RG2, F98, BT4C, RT-2 and CNS-1 Gliomas." *Journal of Neuro-Oncology* 94(3): 299–312.

Beck, Tobias J. et al. 2007. "Interstitial Photodynamic Therapy of Nonresectable Malignant Glioma Recurrences Using 5-Aminolevulinic Acid Induced Protoporphyrin IX." *Lasers in Surgery and Medicine* 39(5): 386–93.

Berg, Kristian, Andreas Dietze, Olav Kaalhus, and Anders Høgset. 2005. "Site-Specific Drug Delivery by Photochemical Internalization Enhances the Antitumor Effect of Bleomycin." *Clinical Cancer Research* 11(23): 8476–85.

Berstad, Maria Brandal, Anette Weyergang, and Kristian Berg. 2012. "Photochemical Internalization (PCI) of HER2-Targeted Toxins: Synergy Is Dependent on the Treatment Sequence." *Biochimica et Biophysica Acta - General Subjects* 1820(12): 1849–58. http://dx.doi.org/10.1016/j.bbagen.2012.08.027.

Bostad, Monica et al. 2013. "Photochemical Internalization (PCI) of Immunotoxins Targeting CD133 Is Specific and Highly Potent at Femtomolar Levels in Cells with Cancer Stem Cell Properties." *Journal of Controlled Release* 168(3): 317–26. http://dx.doi.org/10.1016/j.jconrel.2013.03.023.

Bostad, Monica et al. 2014. "Light-Triggered, Efficient Cytosolic Release of IM7-Saporin Targeting the Putative Cancer Stem Cell Marker CD44 by Photochemical Internalization." *Molecular Pharmaceutics* 11(8): 2764–76.

Chandana, Sreenivasa R., Sujana Movva, Madan Arora, and Trevor Singh. 2008. "Primary Brain Tumors in Adults." *American Family Physician* 77(10): 1423–30.

Chester, A. N., S. Martellucci, and A. M. Scheggi, eds. 1991. "Modelling and Measurements of Light Propagation in Tissue for Diagnostic and Therapeutic Applications." In *Laser Systems for Photobiology and Photomedicine*, NATO ASI Series, Boston, MA: Springer US, 13–27. http://link.springer.com/10.1007/978-1-4684-7287-5.

Christie, Catherine et al. 2017. "Photodynamic Therapy Enhances the Efficacy of Gene-Directed Enzyme Prodrug Therapy." *Photodiagnosis and Photodynamic Therapy* 18: 140–48. http://dx.doi.org/10.1016/j.pdpdt.2017.02.016.

Dietze, a, a Bonsted, a Høgset, and K Berg. 2003. "Photochemical Internalization Enhances the Cytotoxic Effect of the Protein Toxin Gelonin and Transgene Expression in Sarcoma Cells." *Photochemistry and photobiology* 78(3): 283–89. http://www.ncbi.nlm.nih.gov/pubmed/14556316.

Drewinko, B et al. 1976. "Combination Chemotherapy in Vitro with Adriamycin. Observations of Additive, Antagonistic, and Synergistic Effects When Used in Two-Drug Combinations on Cultured Human Lymphoma Cells." *Cancer biochemistry biophysics* 1(4): 187–95. http://www.ncbi.nlm.nih.gov/pubmed/975020.

Dubessy, Christophe, Jean Louis Merlin, Christian Marchal, and François Guillemin. 2000. "Spheroids in Radiobiology and Photodynamic Therapy." *Critical Reviews in Oncology/Hematology* 36(2–3): 179–92.

Eljamel, M. Sam, Carol Goodman, and Harry Moseley. 2008. "ALA and Photofrin® Fluorescence-Guided Resection and Repetitive PDT in Glioblastoma Multiforme: A Single Centre Phase III Randomised Controlled Trial." *Lasers in Medical Science* 23(4): 361–67.

Eng, M S et al. 2018. "Enhanced Targeting of Triple-Negative Breast Carcinoma and Malignant Melanoma by Photochemical Internalization of CSPG4-Targeting Immunotoxins."

Fretz, Marjan M. et al. 2007. "Cytosolic Delivery of Liposomally Targeted Proteins Induced by Photochemical Internalization." *Pharmaceutical Research* 24(11): 2040–47.

Gederaas, O.A. et al. 2017. "Photochemical Internalization in Bladder Cancer-Development of an Orthotopic in Vivo Model." *Photochemical and Photobiological Sciences* 16(11): 1664–76. http://dx.doi.org/10.1039/c7pp00176b.

Godfrey, Nicole. 2018. "Mesothelioma Photodynamic Therapy (PDT)." https://www.mesotheliomaguide.com/treatment/cure/photodynamic-therapy/.

Gonzales, J. et al. 2016. "Focused Ultrasound-Mediated Sonochemical Internalization: An Alternative to Light-Based Therapies." *Journal of Biomedical Optics* 21(7).

Guicciardi, Maria Eugenia, Marcel Leist, and Gregory J. Gores. 2004. "Lysosomes in Cell Death." *Oncogene* 23(16 REV. ISS. 2): 2881–90.

He, Yi-Sheng et al. 2015. "Effects of American Ginseng on Pharmacokinetics of 5-Fluorouracil in Rats." *Biomedical chromatography : BMC* 29(5): 762–67. http://www.ncbi.nlm.nih.gov/pubmed/25339249.

Hirschberg, Henry et al. 2009. "Targeted Delivery of Bleomycin to the Brain Using Photo-Chemical Internalization of Clostridium Perfringens Epsilon Prototoxin." *Journal of Neuro-*

30

Oncology 95(3): 317–29.

Hirschberg, Henry, and Steen J Madsen. 2017. "Synergistic Efficacy of Ultrasound, Sonosensitizers and Chemotherapy: A Review." *Therapeutic Delivery* 8(5): 331–42.

Holland, E. C. 2000. "Glioblastoma Multiforme: The Terminator." *Proceedings of the National Academy of Sciences* 97(12): 6242–44. http://www.pnas.org/cgi/doi/10.1073/pnas.97.12.6242.

Inguscio, Valentina, Elisa Panzarini, and Luciana Dini. 2012. "Autophagy Contributes to the Death/Survival Balance in Cancer PhotoDynamic Therapy." *Cells* 1(3): 464–91. http://www.mdpi.com/2073-4409/1/3/464.

Joy, Beena, S. N. Kumar, A. R. Radhika, and Annie Abraham. 2014. "Embelin (2,5-Dihydroxy-3-Undecyl-p-Benzoquinone) for Photodynamic Therapy: Study of Their Cytotoxicity in Cancer Cells." *Applied Biochemistry and Biotechnology* 175(2): 1069–79.

Kessel, David, M Graça H Vicente, and John J Reiners. 2006. "Initiation of Apoptosis and Autophagy by Photodynamic Therapy." *Autophagy* 2(4): 289–90. http://www.landesbioscience.com/journals/autophagy/article/2792/.

Ko, L., A. Koestner, and W. Wechsler. 1980. "Morphological Characterization of Nitrosourea-Induced Glioma Cell Lines and Clones." *Acta Neuropathologica* 51(1): 23–31.

LaBonia, Gabriel J et al. 2016. "Drug Penetration and Metabolism in 3D Cell Cultures Treated in a 3D Printed Fluidic Device: Assessment of Irinotecan via MALDI Imaging Mass Spectrometry." *Proteomics* 16(11–12): 1814–21. http://www.ncbi.nlm.nih.gov/pubmed/27198560.

Lai, Ping Shan et al. 2008. "Enhanced Cytotoxicity of Saporin by Polyamidoamine Dendrimer Conjugation and Photochemical Internalization." *Journal of Biomedical Materials Research - Part A* 87(1): 147–55.

Liebers, Nora et al. 2017. "Highly Efficient Destruction of Squamous Carcinoma Cells of the Head and Neck by Photochemical Internalization of Ranpirnase." *Journal of experimental therapeutics & oncology* 12(2): 113–20. http://www.ncbi.nlm.nih.gov/pubmed/29161778.

Longley, Daniel B., D. Paul Harkin, and Patrick G. Johnston. 2003. "5-Fluorouracil: Mechanisms of Action and Clinical Strategies." *Nature Reviews Cancer* 3(5): 330–38. http://www.nature.com/doifinder/10.1038/nrc1074.

Lu, Hsueh Lin et al. 2011. "Dendrimer Phthalocyanine-Encapsulated Polymeric Micelle-Mediated Photochemical Internalization Extends the Efficacy of Photodynamic Therapy and Overcomes Drug-Resistance in Vivo." *Journal of Controlled Release* 155(3): 458–64. http://dx.doi.org/10.1016/j.jconrel.2011.06.005.

Madsen, Steen J. et al. 2006. "Multicell Tumor Spheroids in Photodynamic Therapy." *Lasers in Surgery and Medicine* 38(5): 555–64.

Madsen, Steen J. et al. 2009. "Photochemical Internalization Enhances the Efficacy of Bleomycin in Malignant Glioma Cells." In *Proceedings of SPIE*, eds. Nikiforos Kollias et al. , 716132. http://link.aip.org/link/PSISDG/v7161/i1/p716132/s1&Agg=doi.

Madsen, Steen J., Khishigzaya Kharkhuu, and Henry Hirschberg. 2007. "Utility of the F98 Rat Glioma Model for Photodynamic Therapy." *Journal of Environmental Pathology, Toxicology and Oncology* 26(2): 149–55.

De Magalhães, Nzola et al. 2010. "Applications of a New In Vivo Tumor Spheroid Based Shell-Less Chorioallantoic Membrane 3-D Model in Bioengineering Research." *Journal of biomedical science and engineering* 3(1): 20–26. http://www.ncbi.nlm.nih.gov/pubmed/21243108.

Mathews, Marlon S. et al. 2012. "Photochemical Internalization of Bleomycin for Glioma Treatment." *Journal of biomedical optics* 17(5): 058001. http://biomedicaloptics.spiedigitallibrary.org/article.aspx?doi=10.1117/1.JBO.17.5.058001.

Moses, Bio, and Youngjae You. 2013. "Emerging Strategies for Controlling Drug Release by Using Visible/Near IR Light." *Medicinal Chemistry* 03(02): 192–98. https://www.omicsonline.org/emerging-strategies-for-controlling-drug-release-by-using-visiblenear-ir-light-2161-0444.1000138.php?aid=14325.

Muller, Paul J., and Brian C. Wilson. 2006. "Photodynamic Therapy of Brain Tumors—A Work in Progress." *Lasers in Surgery and Medicine* 38(5): 384–89. http://doi.wiley.com/10.1002/lsm.20338.

Muragaki, Yoshihiro et al. 2013. "Phase II Clinical Study on Intraoperative Photodynamic Therapy with Talaporfin Sodium and Semiconductor Laser in Patients with Malignant Brain Tumors." *Journal of Neurosurgery* 119(4): 845–52. http://thejns.org/doi/abs/10.3171/2013.7.JNS13415.

Norum, Ole-Jacob, Karl-Erik Giercksky, and Kristian Berg. 2009. "Photochemical Internalization as an Adjunct to Marginal Surgery in a Human Sarcoma Model." *Photochemical & Photobiological Sciences* 8(6): 758. http://xlink.rsc.org/?DOI=b821129a.

Olsen, Cathrine Elisabeth, Kristian Berg, Pål Kristian Selbo, and Anette Weyergang. 2013. "Circumvention of Resistance to Photodynamic Therapy in Doxorubicin- Resistant Sarcoma by Photochemical Internalization of Gelonin." *Free Radical Biology and Medicine* 65: 1300–1309. http://dx.doi.org/10.1016/j.freeradbiomed.2013.09.010.

Ostrom, Q. T. et al. 2013. "CBTRUS Statistical Report: Primary Brain and Central Nervous System Tumors Diagnosed in the United States in 2006 - 2010." *Journal of Neuro-Oncology* 15(6): 788–96.

Prasmickaite, L et al. 2002. "Photochemical Disruption of Endocytic Vesicles before Delivery of Drugs : A New Strategy for Cancer Therapy." *Br. J. Cancer* 86: 652–57.

Quirk, Brendan J. et al. 2015. "Photodynamic Therapy (PDT) for Malignant Brain Tumors - Where Do We Stand?" *Photodiagnosis and Photodynamic Therapy* 12(3): 530–44. http://dx.doi.org/10.1016/j.pdpdt.2015.04.009.

Reiners, John J. et al. 2010. "Assessing Autophagy in the Context of Photodynamic Therapy." *Autophagy* 6(1): 7–18.

Robertson, C. A., D. Hawkins Evans, and H. Abrahamse. 2009. "Photodynamic Therapy (PDT): A Short Review on Cellular Mechanisms and Cancer Research Applications for PDT."

Journal of Photochemistry and Photobiology B: Biology 96(1): 1–8.
http://dx.doi.org/10.1016/j.jphotobiol.2009.04.001.

Rodriguez, Myriam E. et al. 2009. "Structural Factors and Mechanisms Underlying the Improved Photodynamic Cell Killing with Silicon Phthalocyanine Photosensitizers Directed to Lysosomes versus Mitochondria." *Photochemistry and Photobiology* 85(5): 1189–1200.

Santini, Maria Teresa, Gabriella Rainaldi, and Pietro Luigi Indovina. 2000. "Apoptosis, Cell Adhesion and the Extracellular Matrix in the Three-Dimensional Growth of Multicellular Tumor Spheroids." *Critical Reviews in Oncology/Hematology* 36(2–3): 75–87.

Selbo, Pål K. et al. 2009. "Multi-Modality Therapeutics with Potent Anti-Tumor Effects: Photochemical Internalization Enhances Delivery of the Fusion Toxin ScFvMEL/RGel." *PLoS ONE* 4(8).

Selbo, Pål Kristian, Gowsala Sivam, et al. 2000. "Photochemical Internalisation Increases the Cytotoxic Effect of the Immunotoxin Moc31-Gelonin." *International Journal of Cancer* 87(6): 853–59.

Selbo, Pål Kristian et al. 2010. "Photochemical Internalization Provides Time- and Space-Controlled Endolysosomal Escape of Therapeutic Molecules." *Journal of Controlled Release* 148(1): 2–12. http://dx.doi.org/10.1016/j.jconrel.2010.06.008.

Selbo, Pål Kristian et al. 2012. "Strongly Amphiphilic Photosensitizers Are Not Substrates of the Cancer Stem Cell Marker ABCG2 and Provides Specific and Efficient Light-Triggered Drug Delivery of an EGFR-Targeted Cytotoxic Drug." *Journal of controlled release : official journal of the Controlled Release Society* 159(2): 197–203. http://dx.doi.org/10.1016/j.jconrel.2012.02.003.

Selbo, Pål Kristian, Anders Høgset, Lina Prasmickaite, and Kristian Berg. 2002. "Photochemical Internalisation: A Novel Drug Delivery System." *Tumor Biology* 23(2): 103–12.

Selbo, Pål Kristian, Kirsten Sandvig, Vida Kirveliene, and Kristian Berg. 2000. "Release of Gelonin from Endosomes and Lysosomes to Cytosol by Photochemical Internalization." *Biochimica et Biophysica Acta - General Subjects* 1475(3): 307–13.

Selbo, Pl Kristian et al. 2001. "In Vivo Documentation of Photochemical Internalization, a Novel Approach to Site Specific Cancer Therapy." *International Journal of Cancer* 92(5): 761–66.

Shin, Diane et al. 2018. "Photochemical Internalization Enhanced Macrophage Delivered Chemotherapy." *Photodiagnosis and photodynamic therapy* 21: 156–62. http://www.ncbi.nlm.nih.gov/pubmed/29221858.

Stupp, Roger et al. 2005. "Radiotherapy plus Concomitant and Adjuvant Temozolomide for Glioblastoma." *New England Journal of Medicine* 352(10): 987–96. http://www.nejm.org/doi/abs/10.1056/NEJMoa043330.

Stylli, Stanley S. et al. 2005. "Photodynamic Therapy of High Grade Glioma - Long Term Survival." *Journal of Clinical Neuroscience* 12(4): 389–98.

Sultan, Ahmed A. et al. 2016. "Disulfonated Tetraphenyl Chlorin (TPCS2a)-Induced Photochemical Internalisation of Bleomycin in Patients with Solid Malignancies: A Phase 1,

Dose-Escalation, First-in-Man Trial." *The Lancet Oncology* 17(9): 1217–29.

Tiraby, Michèle et al. 1998. "Concomitant Expression of E. Coli Cytosine Deaminase and Uracil Phosphoribosyltransferase Improves the Cytotoxicity of 5-Fluorocytosine." *FEMS Microbiology Letters* 167(1): 41–49.

Wai, Lam Yip et al. 2007. "Targeted Delivery and Enhanced Cytotoxicity of Cetuximab-Saporin by Photochemical Internalization in EGFR-Positive Cancer Cells." *Molecular Pharmaceutics* 4(2): 241–51.

Wang, Julie T.W. et al. 2012. "Photochemical Internalisation of a Macromolecular Protein Toxin Using a Cell Penetrating Peptide-Photosensitiser Conjugate." *Journal of Controlled Release* 157(2): 305–13. http://dx.doi.org/10.1016/j.jconrel.2011.08.025.

Weyergang, Anette et al. 2011. "Photochemical Internalization of Tumor-Targeted Protein Toxins." *Lasers in Surgery and Medicine* 43(7): 721–33.

Weyergang, Anette, Pål Kristian Selbo, and Kristian Berg. 2006. "Photochemically Stimulated Drug Delivery Increases the Cytotoxicity and Specificity of EGF-Saporin." *Journal of Controlled Release* 111(1–2): 165–73.

Yip, Wai Lam et al. "Targeted Delivery and Enhanced Cytotoxicity of Cetuximab-Saporin by Photochemical Internalization in EGFR-Positive Cancer Cells." *Molecular pharmaceutics* 4(2): 241–51. http://www.ncbi.nlm.nih.gov/pubmed/17263556.

Zaniboni, Alberto, Swapna Prabhu, and Riccardo A. Audisio. 2005. "Chemotherapy and Anaesthetic Drugs: Too Little Is Known." *Lancet Oncology* 6(3): 176–81.

CURRICULUM VITAE

University of Nevada, Las Vegas

School of Allied Health Sciences, Health Physics Department

Karanjit Singh

Email Address:

karanjit.singh42@gmail.com

Degrees:	**B.S., Biomedical Physics** Wayne State University, Detroit, MI.	2013
	Associate, Science North Seattle Community College, Seattle, WA	2009

Thesis Title:

EFFICACY OF COMBINED 5-FLUOROURACIL AND PHOTODYNAMIC THERAPY IN GLIOMA SPHEROIDS